Engineering the Kitaev Spin Liquid in a Quantum Dot System

Tessa Cookmeyer[1,*] and Sankar Das Sarma[2,1]

[1]*Kavli Institute for Theoretical Physics, University of California, Santa Barbara, California 93106-4030, USA*
[2]*Condensed Matter Theory Center and Joint Quantum Institute, Department of Physics, University of Maryland, College Park, Maryland 20742-4111, USA*

The Kitaev model on a honeycomb lattice may provide a robust topological quantum memory platform, but finding a material that realizes the unique spin-liquid phase remains a considerable challenge. We demonstrate that an effective Kitaev Hamiltonian can arise from a half-filled Fermi-Hubbard Hamiltonian where each site can experience a magnetic field in a different direction. As such, we provide a method for realizing the Kitaev spin liquid on a single hexagonal plaquette made up of 12 quantum dots. Despite the small system size, there are clear signatures of the Kitaev spin-liquid ground state, and there is a range of parameters where these signatures are predicted, allowing a potential platform where Kitaev spin-liquid physics can be explored experimentally in quantum dot plaquettes.

Introduction.—Quantum spin liquids are a new phase of matter that exhibit the lack of long-ranged order, an emergent gauge field, long-ranged entanglement, topological order, and fractionalization of spins [1–3]. Despite several promising candidate materials coming from frustrated Kagome [4,5] and triangular [6–10] lattices, there remains a lack of consensus about the nature of their ground-state phase.

Another route to spin-liquid materials comes out of the Kitaev model on the honeycomb lattice [11], an exactly solvable playground for exploring the physics of spin liquids and non-Abelian anyons [12]. In the gapless isotropic phase, the low-energy excitations behave as non-Abelian anyons, once a magnetic field introduces a small gap, and these anyons could form the basis for perfect topological memory [12]. The model became physically relevant after Jackeli and Khaliullin found that certain materials, arising from $4d$ rare earth atoms with the correct geometry, may have a significant Kitaev term [13].

The search for a material realization of the Kitaev spin liquid, a "Kitaev material," has now generated an enormous amount of research on a host of compounds such as Na_2IrO_3 [14–20], Li_2IrO_3 [18,21–23], $H_3LiIr_2O_6$ [24,25], $Na_2Co_2TeO_6$ [26], and α-$RuCl_3$ [27–31]. For $RuCl_3$ in particular, the smoking-gun signature of a Kitaev spin liquid, a quantized thermal Hall effect, has been claimed to have been measured [32–34], but convincingly reproducing the results has been difficult and questions remain [35–37].

Within the Kitaev materials, there remain formidable challenges: most materials enter a long-range ordered phase at low temperature, implying considerable non-Kitaev interactions, and the underlying effective spin Hamiltonian is never known exactly [23,25,38–40], particularly since the fundamental Hamiltonian is an electronic and not a spin Hamiltonian. In fact, it is unclear that naturally occurring solid state materials can manifest the precise Hamiltonian necessary for producing quantum spin liquids described by theoretical models, including the Kitaev model.

There is, however, an alternate way of realizing spin liquids by using engineered structures containing the requisite spin Hamiltonian by design, i.e., quantum simulators. Advances in these systems allow for much more detailed probing of the proposed spin-liquid state. In two-dimensional Rydberg arrays it was theoretically proposed and then experimentally demonstrated that an arrangement of atoms on the bonds of a Kagome lattice can lead to some topological ordering [41,42]. Although the long-ranged nature of the interaction, nonexactness of the Rydberg blockade, and nonequilibrium nature of the state complicate the interpretation of the experiment [41,43,44], this result represents a definitive advance in spin-liquid experiments.

Multiple proposals for realizing Kitaev physics in quantum simulators already exist: the first, using ultracold atoms [45], requires a significant number of independent lasers and two-photon processes and faces serious challenges in cooling the system to low enough temperatures to observe long-ranged topological order [46,47]. More recent work uses an approach based on a Floquet drive [46] and trapped ions [48], but the former requires significant temporal coherence and the latter has stringent constraints on the relevant timescales. There is thus considerable interest in the engineered realization of the Kitaev spin liquid; beyond allowing for the direct access to the physics of spin liquids, topological order, and non-Abelian anyons, the braiding of these anyons would allow for quantum computation with "passive" quantum error correction

[12,49]. Of course, within fully programmable quantum computers it is possible to directly simulate the Kitaev model [50,51] and a similar model with many of the same properties, the toric code [52–54], but these constructions likely benefit less from the topological protection of quantum information.

In this Letter, we discuss how spin-liquid physics can be explored in small quantum-dot systems by precisely creating the Kitaev model on a single hexagonal plaquette (Fig. 1). Quantum-dot systems are a potential spin qubit quantum computing platform where full control has been demonstrated for six sites [55] but where systems with more dots (with as many as 16 having been fabricated so far [56]) can be considered quantum simulators of Hubbard-model physics [57]. In fact, semiconductor quantum-dot-based spin qubits are considered to be a leading quantum computing platform because of their scalability, fast all-electrical operations, and long coherence. Even though the systems are small, they have already provided experimental evidence for Nagaoka ferromagnetism [58–60] and the small-system analog of the Mott transition [61,62], and they could provide evidence for flat-band ferromagnetism in the near future [63,64]. It is already possible to apply a magnetic field gradient using micromagnets [55,65], and our main assumption is that, as the technology improves, it will be possible to place each site in its own effective magnetic field, which is also necessary for quantum computing single qubit operations. Under this assumption, we will derive an effective Hamiltonian that can be tuned to be exactly the Kitaev model on a single hexagon. The physics we propose is no more challenging than fabricating the spin qubit based quantum computing platform, which is a huge activity in more than a dozen research centers and industrial labs including Intel Corporation [66].

Since a "phase" is only defined in the thermodynamic limit, we cannot claim to ever create a Kitaev spin-liquid "phase" in such a small system (which is a problem intrinsic to all quantum simulator platforms). However, we find that the unique properties of the Kitaev model allow for spin-liquid signatures to be manifest even in this small system for a range of parameters around the exact Kitaev point, that is, the system does not have to be perfectly fine-tuned. Our construction is not limited to a single hexagonal plaquette, and can be extended straightforwardly to a many-unit-cell system.

Theory.—We start by explaining the construction on a single hexagonal plaquette, see Fig. 1. In addition to six sites on the vertices of the hexagon, which will interact via an effective Kitaev Hamiltonian, we have an additional six sites that live on the bonds or edges of the hexagon that will be frozen/integrated out. We will demonstrate that this system, which can be fabricated using the existing spin qubit technology, is sufficient to see Kitaev-spin-liquid-like physics.

Parameters ($|t_1| = 1$)

$U \gg |t_1|$

$U \gg |h_B| \gg |t_1|^2/U$

$|t_2| \approx |t_1|^2/(\sqrt{U|h_B|})$

$|h_V| \approx |t_1|^2/U$
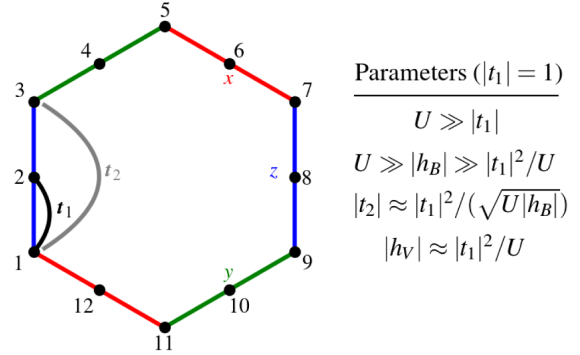
FIG. 1. Our system consists of 12 Fermi-Hubbard sites with interaction strength U arranged on a hexagon as shown. We separate the sites into the odd sites that live on the vertices, V, and the even sites that live on the bonds, B. There is hopping t_1 between all adjacent sites and hopping t_2 between the vertices. Even though a next-nearest-neighbor hopping t_3 between two bond sites should have roughly the same magnitude as t_2, we show in the Supplemental Material (SM) [67] that its effect is $\mathcal{O}(U^{-3})$ and does not alter our construction. The six edges of the hexagon are each given a label, x, y, or z in the pattern indicated by color. The direction of the magnetic field for the bond (vertex) sites points in the direction of the bond label (sum of the two adjacent bond's labels), respectively. For example, $\boldsymbol{h}_4 = -h_B \hat{y}$ and $\boldsymbol{h}_3 = h_V(\hat{z} + \hat{y})$. If $|t_1|, |h_B| \ll U$, $|h_B| \gg |t_1|^2/U$, and $|t_2|$ and $|h_V|$ are related to $|t_1|$, $|h_B|$, and U as shown, then the six vertex spins will interact with an effective Kitaev interaction of strength $K = 2|t_1|^4/(U^2|h_B|)$.

Because we are considering an application to experimental quantum-dot systems, the Hamiltonian for our 12-site system is given, by construction, by the Fermi-Hubbard model in a magnetic field,

$$H = U\sum_i n_{i\uparrow} n_{i\downarrow} + \sum_{ij,\sigma} t_{ij} c_{i\sigma}^\dagger c_{j\sigma} + \frac{1}{2}\sum_{i,\sigma,\sigma'} \boldsymbol{h}_i \cdot c_{i\sigma}^\dagger \boldsymbol{\sigma}_{\sigma,\sigma'} c_{i\sigma'}, \quad (1)$$

where $t_{ij} = t_{ji}^*$ are not necessarily real. We assume that the system is half-filled, which is easy to control in spin qubit quantum-dot structures. We only allow for nearest-neighbor hopping t_1 and hopping between nearest-neighbor vertices t_2, since longer distance hopping falls off exponentially [68]. We are envisioning two different magnetic field strengths: $|h_B|$ for the sites positioned on the edges ("bonds") of the hexagon and $|h_V|$ for sites positioned on the vertices. The direction of the magnetic field follows the pattern described in Fig. 1: each edge is labeled by one of three orthogonal directions, x, y, or z, and the field on a bond site points in that direction (i.e., $\boldsymbol{h}_2 = h_B \hat{z}$), and the field on a vertex points in the sum of the directions of adjacent edges [i.e., $\boldsymbol{h}_1 = h_V(\hat{z} + \hat{x})$]. We use the hopping strength $|t_1|$ as the energy unit. In order to create a single Kitaev plaquette, we will show self-consistently that we need the scalings $U \gg |h_B| \gg |t_1|^2/U$, $|h_V| \sim |t_1|^2/U$, and $|t_2| \sim |t_1|^2/\sqrt{U|h_B|}$. Again, this is, in principle, achievable

in semiconductor spin qubit platforms, where U and the hoppings are the largest and the smallest energy scales, respectively, and the magnetic field is experimentally tunable.

We first perform perturbation theory in $|h_B|/U$, $|t_{ij}|/U$ following [69,70]. The full details of the calculation are given in the SM [67], and we end up with the effective Hamiltonian of localized spins, $\mathbf{S}_i = \boldsymbol{\sigma}_i/2$, at $\mathcal{O}(U^{-3})$:

$$H_{\text{eff,spin}} = \frac{1}{2}\sum_i \left(1 - \frac{2|t_1|^2}{U^2}\right)\mathbf{h}_i \cdot \boldsymbol{\sigma}_i + \sum_{\langle ij \rangle}\frac{|t_1|^2}{U}\left(1 - 4\frac{|t_1|^2}{U^2} + \frac{1}{4}\frac{|h|^2}{U^2}\right)(\boldsymbol{\sigma}_i \cdot \boldsymbol{\sigma}_j - 1) + \sum_{\langle\langle ii' \rangle\rangle_B}\frac{|t_1|^4}{U^3}(\boldsymbol{\sigma}_i \cdot \boldsymbol{\sigma}_{i'} - 1)$$
$$+ \sum_{\langle\langle jk \rangle\rangle_V}\left(\frac{|t_2|^2}{U} + \frac{|t_1|^4}{U^3}\right)(\boldsymbol{\sigma}_j \cdot \boldsymbol{\sigma}_k - 1) + \sum_{\langle ij \rangle}\frac{|t_1|^2}{2U^2}(\mathbf{h}_j \cdot \boldsymbol{\sigma}_i + \mathbf{h}_i \cdot \boldsymbol{\sigma}_j) + 3\sum_{(j,i,k)_B}\sin(\phi_B)\frac{|t_1^2 t_2|}{U^2}\boldsymbol{\sigma}_i \cdot (\boldsymbol{\sigma}_j \times \boldsymbol{\sigma}_k), \quad (2)$$

where $\langle\langle jk \rangle\rangle_V$ ($\langle\langle ii' \rangle\rangle_B$) indicates next-nearest-neighbor pairs between vertex (bond) sites, and $(j, i, k)_B$ indicates a sum over bonds where j, k are the vertex sites and i is the bond site. The value of ϕ_B is how much flux, in units of the flux quantum, pierces the triangle made up of those three sites; in our geometry, $\phi_B = 0$, but in other geometries this term may exist. However, if $\phi_B \ll 1$, this term is likely negligible. Note that we do not have the ring-exchange term

because it requires a four-cycle to exist in hopping. We also have made use of $|h_V| \sim |t_1|^2/U$ and $|t_2| \sim |t_1|^2/\sqrt{U|h_B|}$ to ignore terms that are already higher order in $1/U$.

We now integrate out the bond sites to be left with an effective Hamiltonian for just the vertex sites. We fix the magnetic field on each bond to be $\mathbf{h}_i = -|h_B|\hat{\alpha}$ where site i is on an α bond. We perform perturbation theory in $|t_1|^2/(|h_B|U)$ again to $\mathcal{O}(U^{-3})$ (with $\phi_B = 0$):

$$H_{\text{V,eff}} = \frac{1}{2}\sum_{j \in V}\mathbf{h}_{\text{eff},j} \cdot \boldsymbol{\sigma}_j + \sum_{\langle jk \rangle_{V,\alpha}}J\boldsymbol{\sigma}_j \cdot \boldsymbol{\sigma}_k + K\sigma_j^\alpha\sigma_k^\alpha + C$$

$$\mathbf{h}_{\text{eff},j} = \sum_{i_\alpha \in n.n.(j)}\hat{\alpha}\left[h_V\left(1 - \frac{2|t_1|^2}{U^2}\right) + \frac{2|t_1|^2}{U}\left(1 - 4\frac{|t_1|^2}{U^2} + \frac{|h_B|^2}{4U^2} - \frac{|h_B|}{2U} + 2\frac{|t_1|^2}{U|h_B|}\right)\right]$$

$$J = \frac{|t_2|^2}{U} + \frac{|t_1|^4}{U^3} - 2\frac{|t_1|^4}{U^2|h_B|} + 2\frac{|t_1|^4 h_V}{U^2|h_B|^2} - 4\frac{|t_1|^6}{U^3|h_B|^2} \qquad K = 2\frac{|t_1|^4}{U^2|h_B|} - 4\frac{|t_1|^4 h_V}{U^2|h_B|^2} + 8\frac{|t_1|^6}{U^3|h_B|^2}, \quad (3)$$

where $\langle jk \rangle_{V,\alpha}$ indicates nearest-neighbor pairs of vertices that are connected via an α bond, and $i_\alpha \in n.n.(j)$ indicates the nearest neighbors of site j that are on an α bond. The constant C is provided in the SM [67].

Since we want the field strength, $|h_{\text{eff},j}/K \lesssim 1$ and Heisenberg coupling $J/K \lesssim 1$, we need $|t_2| \lesssim \sqrt{2}|t_1|^2/\sqrt{U|h_B|}$ and $h_V \approx -2|t_1|^2/U$, which justifies the scaling we used to derive Eqs. (2) and (3). Although we have computed expressions for these quantities to $\mathcal{O}(U^{-3})$, we see that the Kitaev coupling is $\mathcal{O}(U^{-2})$ implying that, even if $\phi_B = 0$ turns out to be a poor assumption, our construction still works for large enough U.

Despite the notion of a phase being properly defined only in the thermodynamic limit, there is a clear-cut signature of a Kitaev spin-liquid-like "phase" even in this small plaquette. First, there is an operator defined on each plaquette that commutes with the Kitaev Hamiltonian. For our single plaquette, it is given by

$$W_P = \sigma_1^y\sigma_3^x\sigma_5^z\sigma_7^y\sigma_9^x\sigma_{11}^z = \pm 1, \quad (4)$$

where the site indices are from Fig. 1. The value of $W_P = \pm 1$ is a signature of the emergent $\mathbb{Z}_2$ gauge field of the Kitaev model [11]. Second, the spin-spin correlators are short-ranged [71]: the only nonzero static $S^z - S^z$ correlators for our system at the Kitaev point are $\langle S_1^z S_3^z \rangle = \langle S_7^z S_9^z \rangle = -1/6$ and $\langle S_j^z S_j^z \rangle = 1/4$ with $\mathbf{S} = \boldsymbol{\sigma}/2$.

Results.—In order to verify our theory and clarify possible experimental signatures, we use the density matrix renormalization group (DMRG) [72] method to directly find the ground state of Eq. (1) and compare with exact diagonalization (ED) on six sites given by Eq. (3). For DMRG, we use TeNPy [73] with a bond dimension of $\chi = 4096$, large enough to describe the ground state exactly.

In Fig. 2, we plot the plaquette operator, $\langle W_P \rangle$, and $\langle S_i^z S_j^z \rangle$ for a z bond $(i = 1, j = 3)$, an x bond $(i = 1, j = 11)$, and the farthest spins $(i = 1, j = 7)$. We set $t_1 = h_B = 1$ with t_2 and h_V given by
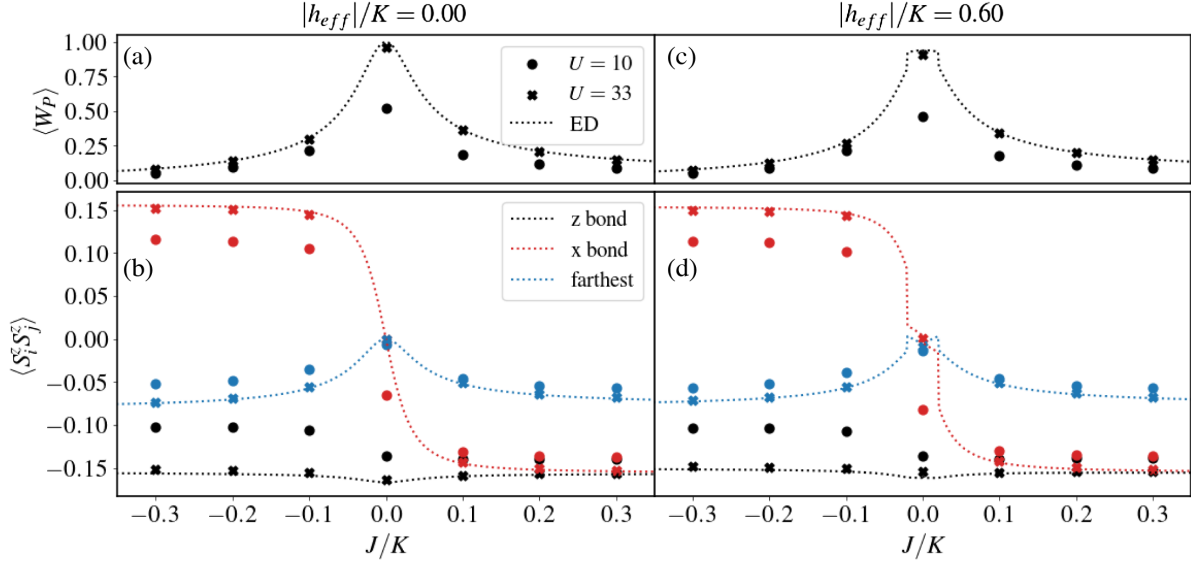
FIG. 2. We perform DMRG on twelve Fermi-Hubbard sites at half filling (scatter plot points) as well as exact diagonalization (ED) on six spin-1/2 sites using the effective Hamiltonian, Eq. (3). We set $t_1 = h_B = 1$, and the values of t_2 and h_V are set so as to give a specified value of J/K and h_{eff} via Eq. (5). In (a), (b) $|h_{\text{eff}}|/K = 0$ and in (c),(d) $|h_{\text{eff}}|/K = 0.6$ and the value of J/K is indicated on the horizontal axis. In all plots, the value of U used for DMRG is $U = 10$ ($U = 33$) for the circle (×) points, respectively. By $U = 33$, the DMRG results are almost entirely on top of the ED curves showing that the effective Hamiltonian is a Heisenberg-Kitaev Hamiltonian in a magnetic field. We compare two observables: in (a), (c), we plot the plaquette operator Eq. (4) and in (c),(d) we plot the correlator $\langle S_i^z S_j^z \rangle$ for a z bond ($i = 1, j = 3$), an x bond ($i = 1, j = 11$), and the farthest spins ($i = 1, j = 7$). In (b) and (d), the color of the points and dashed line indicates which spin correlator is being plotted. A Kitaev plaquette would have $W_P = 1$ and the x bond and farthest spin correlators will be zero. Clearly $J/K = 0$ and $|h_{\text{eff}}|/K = 0$ satisfy these requirements, but when $|h_{\text{eff}}|/K \neq 0$, there is a small range of J/K where these are approximately true as well.

$$h_V = \frac{-A_1 + A_2 \frac{h_{\text{eff}}}{K}}{A_3 + 4A_4 \frac{h_{\text{eff}}}{K}},$$

$$t_2 = \pm\sqrt{U\left(\frac{J}{K}(A_2 - 4A_4 h_V) - 2A_4 h_V - A_5\right)},$$

$$A_1 = 2\frac{|t_1|^2}{U}\left(1 + \frac{h_B^2 - 16|t_1|^2}{4U^2} + \frac{4|t_1|^2 - h_B^2}{2U|h_B|}\right),$$

$$A_2 = \frac{2|t_1|^4}{U^2|h_B|} + 8\frac{|t_1|^6}{U^3 h_B^2}, \qquad A_3 = 1 - 2\frac{|t_1|^2}{U^2},$$

$$A_4 = \frac{|t_1|^4}{U^2 h_B^2}, \qquad A_5 = \frac{|t_1|^4}{U^3} - 2\frac{|t_1|^4}{U^2|h_B|} - \frac{4|t_1|^6}{U^3 h_B^2}, \qquad (5)$$

so as to reproduce a targeted value of J/K and $|h_{\text{eff}}|/K$ with errors at higher order than $\mathcal{O}(U^{-3})$. We are able to verify that DMRG and ED have ground-state energies that agree to $\mathcal{O}(U^{-4})$ when the parameters are specified in this way (see SM [67]). We use real values of the hoppings so as to avoid additional parameters needed to compute the flux, ϕ_B.

We see that when $U/|t_1| = 33$, the two methods give excellent agreement with each other further lending credence to our theoretical derivations and plaquette constructions efficacy. Note that, when $|h_{\text{eff}}|/K = 0$ and $J/K \ll 1$, $\langle W_P \rangle$ and $\langle S_i^z S_j^z \rangle$ take on their approximate

values as expected for the Kitaev model. Additionally, when $|h_{\text{eff}}|/K \neq 0$, there are points where the derivatives of these observables are discontinuous, and, in the region $J/K \ll 1$, they take a value close to the Kitaev value. In a large system, these features are consistent with the magnetic field gapping out the itinerant Majoranas and providing a gap that J must overcome; in our system, we have verified that some of the degeneracy seen at the J/K, $|h_{\text{eff}}|/K = 0$ point is lifted in the presence of a magnetic field implying that the same interpretation might hold.

Taken together, the numerics demonstrate that, even though strictly speaking the Kitaev Hamiltonian only arises at a single point, it is possible to see evidence of the Kitaev state in a range of parameters meaning that the construction is less fine-tuned than anticipated, i.e., there is some robustness.

Conclusion.—In this Letter, we proposed how to realize the Kitaev honeycomb model, with its non-Abelian anyons, topological order, and its potential as a quantum memory platform with topologically protected quantum information, on connected quantum dots; these small spin qubit arrays have already been successfully used as experimental platforms to study many-body collective phenomena such as Mott-Hubbard transitions [61,62] and Nagaoka ferromagnetism [58–60], making our work both timely and experimentally relevant.

From the above results (and additional numerical results shown in [67]), we argue that if $|J|/K \lesssim 0.02$ and $|h_{\text{eff}}|/K \lesssim 0.75$, our 12-site system should exhibit Kitaev-spin-liquid-like physics. The experimental setup therefore does not need to be perfectly fine-tuned to observe this physics: for $U/|t_1| = 33$ and $|t_1|/|h_B| = 1$, these values roughly correspond to a range of $0.0615 \leq h_V \leq 0.0650$ and $0.2565 \leq t_2 \leq 0.2620$ with $K \approx 0.00229$. This range reveals that h_V and t_2 need only be accurate at the 5% and 2% level, respectively, which should be experimentally controllable in semiconductor quantum-dot structures. It is also not necessary to prepare the ground state of the system. As long as the energy is well below $|h_B|$, the state will always have short-ranged spin-spin correlators as this property is true for every eigenstate in the Kitaev model [71].

Our proposal, though developed for a single plaquette, works for systems of as many connected plaquettes as is desired. Our expressions can be straightforwardly generalized to include an arbitrary system size or geometry, and we include fully general expressions in the SM [67] [the only change to Eq. (3) is to the coefficient of the $h_V|t_1|^2/U^2$ term]. An advantage to having several plaquettes connected to each other is that, for all interior vertex sites (i.e., those sites with a neighbor along an x, y, and z bond), the applied field on those sites will all be in the $\hat{x} + \hat{y} + \hat{z}$ direction and will therefore be uniform. Alternatively, another advantage of our construction is that the field on the vertex sites does not need to be tuned individually. If the field on the bond sites decays at just the right rate, it can provide the necessary field as $\boldsymbol{h}_{j \in V}$ points in the same direction as the sum of the neighboring $\boldsymbol{h}_{j \in B}$.

The most significant perturbation we have not explicitly included in this Letter is a hopping between nearest-neighbor bond sites, t_3, that is similar in strength to t_2. As is shown in the SM [67], the only change to our effective Hamiltonian (besides a constant energy shift) due to this addition is an effective field on the vertex sites at $\mathcal{O}(U^{-3})$. These terms slightly change the direction of the magnetic field that needs to be applied to a vertex site if the vertex site is not in the interior of the system, but it can be canceled if the field on each vertex site can be tuned individually.

The main experimental difficulty in our proposal is realizing individual magnetic fields on each bond site. In the SM [67], we consider what happens if the magnitude and direction of these fields are not perfectly tuned. If the error in the magnitude is $\mathcal{O}(1/U)$ and if the components of the field of the bond site pointing in the incorrect direction (e.g., in the $\hat{x}$ and $\hat{y}$ directions for the $\hat{z}$ bond) are less than $|t_1|^2/(10U)$, we find some amount of robustness of our chosen signal of spin-liquid physics for the ground state, but large enough inaccuracies will wash out the signal.

Although our proposal should realize a Kitaev spin-liquid plaquette in principle, there are many open questions. For example, what are the necessary conditions and system sizes to observe the non-Abelian anyon braiding signatures? What are the most suitable experimental signatures of these anyons? How does one realize topological qubits using anyon braiding in such Kitaev plaquettes? Our work should motivate both experimental work to realize our proposed Kitaev quantum-dot plaquette and theoretical work to answer these questions.

*Corresponding author: tcookmeyer@kitp.ucsb.edu

[1] L. Savary and L. Balents, Quantum spin liquids: A review, Rep. Prog. Phys. **80**, 016502 (2016).

[2] J. Wen, S.-L. Yu, S. Li, W. Yu, and J.-X. Li, Experimental identification of quantum spin liquids, npj Quantum Mater. **4**, 12 (2019).

[3] C. Broholm, R. Cava, S. Kivelson, D. Nocera, M. Norman, and T. Senthil, Quantum spin liquids, Science **367**, eaay0668 (2020).

[4] Z. Feng, Z. Li, X. Meng, W. Yi, Y. Wei, J. Zhang, Y.-C. Wang, W. Jiang, Z. Liu, S. Li *et al.*, Gapped spin-1/2 spinon excitations in a new kagome quantum spin liquid compound $Cu_3Zn(OH)_6FBr$, Chin. Phys. Lett. **34**, 077502 (2017).

[5] M. P. Shores, E. A. Nytko, B. M. Bartlett, and D. G. Nocera, A structurally perfect $s = 1/2$ kagome antiferromagnet, J. Am. Chem. Soc. **127**, 13462 (2005).

[6] Y. Shimizu, K. Miyagawa, K. Kanoda, M. Maesato, and G. Saito, Spin liquid state in an organic Mott insulator with a triangular lattice, Phys. Rev. Lett. **91**, 107001 (2003).

[7] T. Itou, A. Oyamada, S. Maegawa, M. Tamura, and R. Kato, Quantum spin liquid in the spin-1/2 triangular antiferromagnet $EtMe_3Sb[Pd(dmit)_2]_2$, Phys. Rev. B **77**, 104413 (2008).

[8] K. T. Law and P. A. Lee, 1T-TaS_2 as a quantum spin liquid, Proc. Natl. Acad. Sci. U.S.A. **114**, 6996 (2017).

[9] W.-Y. He, X. Y. Xu, G. Chen, K. T. Law, and P. A. Lee, Spinon Fermi surface in a cluster Mott insulator model on a triangular lattice and possible application to $1T - TaS_2$, Phys. Rev. Lett. **121**, 046401 (2018).

[10] S. Xu, R. Bag, N. E. Sherman, L. Yadav, A. I. Kolesnikov, A. A. Podlesnyak, J. E. Moore, and S. Haravifard,

Realization of U(1) Dirac quantum spin liquid in YbZn$_2$GaO$_5$, arXiv:2305.20040.

[11] A. Kitaev, Anyons in an exactly solved model and beyond, Ann. Phys. (Amsterdam) **321**, 2 (2006).

[12] C. Nayak, S. H. Simon, A. Stern, M. Freedman, and S. Das Sarma, Non-Abelian anyons and topological quantum computation, Rev. Mod. Phys. **80**, 1083 (2008).

[13] G. Jackeli and G. Khaliullin, Mott insulators in the strong spin-orbit coupling limit: From Heisenberg to a quantum compass and Kitaev models, Phys. Rev. Lett. **102**, 017205 (2009).

[14] F. Ye, S. Chi, H. Cao, B. C. Chakoumakos, J. A. Fernandez-Baca, R. Custelcean, T. F. Qi, O. B. Korneta, and G. Cao, Direct evidence of a zigzag spin-chain structure in the honeycomb lattice: A neutron and x-ray diffraction investigation of single-crystal Na$_2$IrO$_3$, Phys. Rev. B **85**, 180403(R) (2012).

[15] R. Comin, G. Levy, B. Ludbrook, Z.-H. Zhu, C. N. Veenstra, J. A. Rosen, Y. Singh, P. Gegenwart, D. Stricker, J. N. Hancock, D. van der Marel, I. S. Elfimov, and A. Damascelli, Na$_2$IrO$_3$ as a novel relativistic mott insulator with a 340-MeV gap, Phys. Rev. Lett. **109**, 266406 (2012).

[16] S. Hwan Chun, J.-W. Kim, J. Kim, H. Zheng, C. C. Stoumpos, C. Malliakas, J. Mitchell, K. Mehlawat, Y. Singh, Y. Choi *et al.*, Direct evidence for dominant bond-directional interactions in a honeycomb lattice iridate Na$_2$IrO$_3$, Nat. Phys. **11**, 462 (2015).

[17] Y. Singh and P. Gegenwart, Antiferromagnetic Mott insulating state in single crystals of the honeycomb lattice material Na$_2$IrO$_3$, Phys. Rev. B **82**, 064412 (2010).

[18] Y. Singh, S. Manni, J. Reuther, T. Berlijn, R. Thomale, W. Ku, S. Trebst, and P. Gegenwart, Relevance of the Heisenberg-Kitaev model for the honeycomb lattice iridates A_2IrO$_3$, Phys. Rev. Lett. **108**, 127203 (2012).

[19] S. K. Choi, R. Coldea, A. N. Kolmogorov, T. Lancaster, I. I. Mazin, S. J. Blundell, P. G. Radaelli, Y. Singh, P. Gegenwart, K. R. Choi, S.-W. Cheong, P. J. Baker, C. Stock, and J. Taylor, Spin waves and revised crystal structure of honeycomb iridate Na$_2$IrO$_3$, Phys. Rev. Lett. **108**, 127204 (2012).

[20] X. Liu, T. Berlijn, W.-G. Yin, W. Ku, A. Tsvelik, Y.-J. Kim, H. Gretarsson, Y. Singh, P. Gegenwart, and J. P. Hill, Long-range magnetic ordering in Na$_2$IrO$_3$, Phys. Rev. B **83**, 220403(R) (2011).

[21] S. C. Williams, R. D. Johnson, F. Freund, S. Choi, A. Jesche, I. Kimchi, S. Manni, A. Bombardi, P. Manuel, P. Gegenwart, and R. Coldea, Incommensurate counterrotating magnetic order stabilized by Kitaev interactions in the layered honeycomb $\alpha - Li_2IrO_3$, Phys. Rev. B **93**, 195158 (2016).

[22] A. Biffin, R. D. Johnson, I. Kimchi, R. Morris, A. Bombardi, J. G. Analytis, A. Vishwanath, and R. Coldea, Noncoplanar and counterrotating incommensurate magnetic order stabilized by kitaev interactions in $\gamma - Li_2IrO_3$, Phys. Rev. Lett. **113**, 197201 (2014).

[23] S. M. Winter, Y. Li, H. O. Jeschke, and R. Valentí, Challenges in design of Kitaev materials: Magnetic interactions from competing energy scales, Phys. Rev. B **93**, 214431 (2016).

[24] K. Kitagawa, T. Takayama, Y. Matsumoto, A. Kato, R. Takano, Y. Kishimoto, S. Bette, R. Dinnebier, G. Jackeli, and H. Takagi, A spin–orbital-entangled quantum liquid on a honeycomb lattice, Nature (London) **554**, 341 (2018).

[25] H. Takagi, T. Takayama, G. Jackeli, G. Khaliullin, and S. E. Nagler, Concept and realization of Kitaev quantum spin liquids, Nat. Rev. Phys. **1**, 264 (2019).

[26] G. Lin, J. Jeong, C. Kim, Y. Wang, Q. Huang, T. Masuda, S. Asai, S. Itoh, G. Günther, M. Russina *et al.*, Field-induced quantum spin disordered state in spin-1/2 honeycomb magnet Na$_2$Co$_2$TeO$_6$, Nat. Commun. **12**, 5559 (2021).

[27] A. Banerjee, P. Lampen-Kelley, J. Knolle, C. Balz, A. A. Aczel, B. Winn, Y. Liu, D. Pajerowski, J. Yan, C. A. Bridges *et al.*, Excitations in the field-induced quantum spin liquid state of α-RuCl$_3$, npj Quantum Mater. **3**, 8 (2018).

[28] A. Banerjee, J. Yan, J. Knolle, C. A. Bridges, M. B. Stone, M. D. Lumsden, D. G. Mandrus, D. A. Tennant, R. Moessner, and S. E. Nagler, Neutron scattering in the proximate quantum spin liquid $\alpha - $RuCl$_3$, Science **356**, 1055 (2017).

[29] A. Banerjee, C. Bridges, J.-Q. Yan, A. Aczel, L. Li, M. Stone, G. Granroth, M. Lumsden, Y. Yiu, J. Knolle *et al.*, Proximate Kitaev quantum spin liquid behaviour in a honeycomb magnet, Nat. Mater. **15**, 733 (2016).

[30] K. Ran, J. Wang, W. Wang, Z.-Y. Dong, X. Ren, S. Bao, S. Li, Z. Ma, Y. Gan, Y. Zhang, J. T. Park, G. Deng, S. Danilkin, S.-L. Yu, J.-X. Li, and J. Wen, Spin-wave excitations evidencing the Kitaev interaction in single crystalline $\alpha - $RuCl$_3$, Phys. Rev. Lett. **118**, 107203 (2017).

[31] J. Nasu, J. Knolle, D. L. Kovrizhin, Y. Motome, and R. Moessner, Fermionic response from fractionalization in an insulating two-dimensional magnet, Nat. Phys. **12**, 912 (2016).

[32] Y. Kasahara, T. Ohnishi, Y. Mizukami, O. Tanaka, S. Ma, K. Sugii, N. Kurita, H. Tanaka, J. Nasu, Y. Motome *et al.*, Majorana quantization and half-integer thermal quantum Hall effect in a Kitaev spin liquid, Nature (London) **559**, 227 (2018).

[33] T. Yokoi, S. Ma, Y. Kasahara, S. Kasahara, T. Shibauchi, N. Kurita, H. Tanaka, J. Nasu, Y. Motome, C. Hickey *et al.*, Half-integer quantized anomalous thermal Hall effect in the Kitaev material candidate α-RuCl$_3$, Science **373**, 568 (2021).

[34] J. Bruin, R. Claus, Y. Matsumoto, N. Kurita, H. Tanaka, and H. Takagi, Robustness of the thermal Hall effect close to half-quantization in α-RuCl$_3$, Nat. Phys. **18**, 401 (2022).

[35] M. Yamashita, J. Gouchi, Y. Uwatoko, N. Kurita, and H. Tanaka, Sample dependence of half-integer quantized thermal Hall effect in the Kitaev spin-liquid candidate α-RuCl$_3$, Phys. Rev. B **102**, 220404(R) (2020).

[36] P. Czajka, T. Gao, M. Hirschberger, P. Lampen-Kelley, A. Banerjee, N. Quirk, D. G. Mandrus, S. E. Nagler, and N. Ong, The planar thermal Hall conductivity in the Kitaev magnet α-RuCl$_3$, Nat. Mater. **22**, 36 (2023).

[37] É. Lefrançois, G. Grissonnanche, J. Baglo, P. Lampen-Kelley, J. Yan, C. Balz, D. Mandrus, S. Nagler, S. Kim, Y.-J. Kim *et al.*, Evidence of a phonon Hall effect in the Kitaev spin liquid candidate α-RuCl$_3$, Phys. Rev. X **12**, 021025 (2022).

[38] A. M. Samarakoon, P. Laurell, C. Balz, A. Banerjee, P. Lampen-Kelley, D. Mandrus, S. E. Nagler, S. Okamoto, and D. A. Tennant, Extraction of the interaction parameters for α-RuCl$_3$ from neutron data using machine learning, Phys. Rev. Res. **4**, L022061 (2022).

[39] P. A. Maksimov and A. L. Chernyshev, Rethinking α-RuCl$_3$, Phys. Rev. Res. **2**, 033011 (2020).

[40] K. Slagle, W. Choi, L. E. Chern, and Y. B. Kim, Theory of a quantum spin liquid in the hydrogen-intercalated honeycomb iridate H$_3$LiIr$_2$O$_6$, Phys. Rev. B **97**, 115159 (2018).

[41] R. Verresen, M. D. Lukin, and A. Vishwanath, Prediction of toric code topological order from Rydberg blockade, Phys. Rev. X **11**, 031005 (2021).

[42] G. Semeghini, H. Levine, A. Keesling, S. Ebadi, T. T. Wang, D. Bluvstein, R. Verresen, H. Pichler, M. Kalinowski, R. Samajdar *et al.*, Probing topological spin liquids on a programmable quantum simulator, Science **374**, 1242 (2021).

[43] G. Giudici, M. D. Lukin, and H. Pichler, Dynamical preparation of quantum spin liquids in Rydberg atom arrays, Phys. Rev. Lett. **129**, 090401 (2022).

[44] R. Sahay, A. Vishwanath, and R. Verresen, Quantum spin puddles and lakes: NISQ-era spin liquids from non-equilibrium dynamics, arXiv:2211.01381.

[45] L.-M. Duan, E. Demler, and M. D. Lukin, Controlling spin exchange interactions of ultracold atoms in optical lattices, Phys. Rev. Lett. **91**, 090402 (2003).

[46] B.-Y. Sun, N. Goldman, M. Aidelsburger, and M. Bukov, Engineering and probing non-Abelian chiral spin liquids using periodically driven ultracold atoms, PRX Quantum **4**, 020329 (2023).

[47] L. Tarruell and L. Sanchez-Palencia, Quantum simulation of the Hubbard model with ultracold fermions in optical lattices, C.R. Phys. **19**, 365 (2018).

[48] R. Schmied, J. H. Wesenberg, and D. Leibfried, Quantum simulation of the hexagonal Kitaev model with trapped ions, New J. Phys. **13**, 115011 (2011).

[49] B. M. Terhal, Quantum error correction for quantum memories, Rev. Mod. Phys. **87**, 307 (2015).

[50] X. Xiao, J. K. Freericks, and A. F. Kemper, Determining quantum phase diagrams of topological Kitaev-inspired models on NISQ quantum hardware, Quantum **5**, 553 (2021).

[51] T. A. Bespalova and O. Kyriienko, Quantum simulation and ground state preparation for the honeycomb Kitaev model, arXiv:2109.13883.

[52] C.-Y. Lu, W.-B. Gao, O. Gühne, X.-Q. Zhou, Z.-B. Chen, and J.-W. Pan, Demonstrating anyonic fractional statistics with a six-qubit quantum simulator, Phys. Rev. Lett. **102**, 030502 (2009).

[53] Y.-J. Han, R. Raussendorf, and L.-M. Duan, Scheme for demonstration of fractional statistics of anyons in an exactly solvable model, Phys. Rev. Lett. **98**, 150404 (2007).

[54] S. Xu, Z.-Z. Sun, K. Wang, L. Xiang, Z. Bao, Z. Zhu, F. Shen, Z. Song, P. Zhang, W. Ren *et al.*, Digital simulation of projective non-Abelian anyons with 68 superconducting qubits, Chin. Phys. Lett. **40**, 060301 (2023).

[55] S. G. Philips, M. T. Madzik, S. V. Amitonov, S. L. de Snoo, M. Russ, N. Kalhor, C. Volk, W. I. Lawrie, D. Brousse, L. Tryputen *et al.*, Universal control of a six-qubit quantum processor in silicon, Nature (London) **609**, 919 (2022).

[56] F. Borsoi, N. W. Hendrickx, V. John, M. Meyer, S. Motz, F. van Riggelen, A. Sammak, S. L. de Snoo, G. Scappucci, and M. Veldhorst, Shared control of a 16 semiconductor quantum dot crossbar array, Nat. Nanotechnol. **19**, 21 (2023).

[57] D. Buterakos and S. D. Sarma, Magnetic phases of bilayer quantum-dot Hubbard model plaquettes, Phys. Rev. B **108**, 235301 (2023).

[58] Y. Nagaoka, Ferromagnetism in a narrow, almost half-filled s band, Phys. Rev. **147**, 392 (1966).

[59] J. P. Dehollain, U. Mukhopadhyay, V. P. Michal, Y. Wang, B. Wunsch, C. Reichl, W. Wegscheider, M. S. Rudner, E. Demler, and L. M. Vandersypen, Nagaoka ferromagnetism observed in a quantum dot plaquette, Nature (London) **579**, 528 (2020).

[60] D. Buterakos and S. Das Sarma, Ferromagnetism in quantum dot plaquettes, Phys. Rev. B **100**, 224421 (2019).

[61] T. Hensgens, T. Fujita, L. Janssen, X. Li, C. Van Diepen, C. Reichl, W. Wegscheider, S. Das Sarma, and L. M. Vandersypen, Quantum simulation of a Fermi–Hubbard model using a semiconductor quantum dot array, Nature (London) **548**, 70 (2017).

[62] C. A. Stafford and S. Das Sarma, Collective coulomb blockade in an array of quantum dots: A Mott-Hubbard approach, Phys. Rev. Lett. **72**, 3590 (1994).

[63] H. Tasaki, Ferromagnetism in the Hubbard models with degenerate single-electron ground states, Phys. Rev. Lett. **69**, 1608 (1992).

[64] D. Buterakos and S. Das Sarma, Certain exact many-body results for Hubbard model ground states testable in small quantum dot arrays, Phys. Rev. B **107**, 014403 (2023).

[65] M. Pioro-Ladriere, Y. Tokura, T. Obata, T. Kubo, and S. Tarucha, Micromagnets for coherent control of spin-charge qubit in lateral quantum dots, Appl. Phys. Lett. **90**, 024105 (2007).

[66] S. Neyens, O. Zietz, T. Watson, F. Luthi, A. Nethwewala, H. George, E. Henry, A. Wagner, M. Islam, R. Pillarisetty *et al.*, Probing single electrons across 300 mm spin qubit wafers, arXiv:2307.04812.

[67] See Supplemental Material at http://link.aps.org/supplemental/10.1103/PhysRevLett.132.186501 for the perturbation theory details, additional numerical results, and a discussion of the addition of a nearest-neighbor hopping between bond sites and imperfectly applied magnetic fields.

[68] Although the hopping t_3 between nearest-neighbor bond sites is of the same order as t_2, it produces only a small change in the effective magnetic field of the vertex sites at $\mathcal{O}(U^{-3})$. See the SM [67].

[69] M. Takahashi, Half-filled Hubbard model at low temperature, J. Phys. C **10**, 1289 (1977).

[70] A. H. MacDonald, S. M. Girvin, and D. Yoshioka, (t/U) expansion for the Hubbard model, Phys. Rev. B **37**, 9753 (1988).

[71] G. Baskaran, S. Mandal, and R. Shankar, Exact results for spin dynamics and fractionalization in the Kitaev model, Phys. Rev. Lett. **98**, 247201 (2007).

[72] S. R. White, Density matrix formulation for quantum renormalization groups, Phys. Rev. Lett. **69**, 2863 (1992).

[73] J. Hauschild and F. Pollmann, Efficient numerical simulations with tensor networks: Tensor network PYTHON (TeNPy), SciPost Phys. Lect. Notes **5** (2018), code available from https://github.com/tenpy/tenpy.